SERS—a single-molecule and nanoscale tool for bioanalytics

Janina Kneipp,*[ab] Harald Kneipp[a] and Katrin Kneipp[ac]

Received 13th March 2008
First published as an Advance Article on the web 20th March 2008
DOI: 10.1039/b708459p

Surface enhanced Raman scattering (SERS) at extremely high enhancement level turns the weak inelastic scattering effect of photons on vibrational quantum states into a structurally sensitive single-molecule and nanoscale probe. The effect opens up exciting opportunities for applications of vibrational spectroscopy in biology. The concept of SERS can be extended to two-photon excitation by exploiting surface enhanced hyper-Raman scattering (SEHRS). This *critical review* introduces the physics behind single-molecule SERS and discusses the capabilities of the effect in bioanalytics (100 references).

1 Introduction

Raman scattering occurs during inelastic collision of photons with molecules.[1,2] In this scattering process, photons may gain energy from, or lose it to, the molecules. A change in the photon energy must produce a change in the frequency $\Delta\nu = \Delta E/h$ resulting in scattered photons $h\nu_S$ shifted in frequency relative to the excitation photons $h\nu_L$ by the energy of characteristic molecular vibrations $h\nu_M$. Therefore, a Raman spectrum comprising several different "Raman lines" generated by scattering from different molecular vibrations provides a vibrational "fingerprint" of a molecule.

Fig. 1 illustrates the Raman scattering (RS) process in a molecular level scheme. Depending on whether photons interact with a molecule in its vibrational ground or first excited vibrational state, the scattering signals appear at the low energy side (Stokes: $h\nu_S = h\nu_L - h\nu_M$) or high energy side (anti-Stokes: $h\nu_{aS} = h\nu_L + h\nu_M$) of the excitation laser. The scattering signal power P_{RS} of a Raman line depends on excitation intensity I_L and the Raman cross section σ^R, where σ^R is determined by the polarizability derivative of the molecular vibration. In general, anti-Stokes Raman scattering results in much lower scattering signals compared to Stokes scattering, because only a small fraction of molecules, determined by the Boltzmann population is in an excited vibrational state and can contribute to anti-Stokes Raman scattering.

In hyper-Raman scattering (HRS) two-photons are simultaneously scattered, and thus HRS results in Raman signals shifted relative to the doubled energy of the excitation laser ($h\nu_{HS} = 2h\nu_L - h\nu_M$ and $h\nu_{HaS} = 2h\nu_L + h\nu_M$).[3] HRS follows symmetry selection rules different from regular one-photon RS, and therefore it can probe vibrational modes complementary to those that appear in a "normal" RS spectrum. The power of RS signals P_{RS} is linearly dependent on the excitation intensity whereas HRS signals depends on the on the excitation intensity to the power of two.

Raman scattering is a very weak effect. Typical Raman cross section are between 10^{-30}–10^{-25} cm^2 per molecule with the larger values occurring only under favorable resonance-Raman conditions when the excitation light matches the related electronic transition energy in the molecule. For comparison, fluorescence spectroscopy exploits effective cross sections between 10^{-17} cm^2 and 10^{-16} cm^2. To achieve adequate conversion rates from excitation laser photons to Raman photons, the small Raman cross sections require a large number of molecules. Therefore, in general, Raman spectroscopy has been considered a technique for structural analysis, rather than a method for ultra-sensitive trace detection or even as tool for single-molecule probing.[4]

Hyper-Raman scattering as a two-photon excited process is a lot weaker than even one-photon excited Raman scattering. Cross sections on the order of 10^{-65} cm^{4}s, 35 orders of magnitude smaller than cross sections of Raman scattering and 15 orders of

[a] *Harvard University Medical School, Wellman Center for Photomedicine, Boston, MA 02114, USA. E-mail: kneipp@usa.net*
[b] *Federal Institute for Materials Research and Testing, D-12489 Berlin, Germany. E-mail: jkneipp@janina-kneipp.de*
[c] *Harvard-MIT Division of Health Sciences and Technology, Cambridge, MA 02139, USA*

Janina Kneipp received her Diploma in Biology and after thesis work at Robert-Koch-Institut a PhD from Free University Berlin in 2002. During her postdoctoral studies she worked at Princeton University's Chemistry Department and conducted research at Harvard Medical School. Her current research is focused on the development of novel sensitive vibrational spectroscopic methods to investigate small-scale complex biomaterials.

Harald Kneipp received his Diploma in Physics from Friedrich Schiller University in Jena, and a PhD degree in Physics from the Academy of Sciences in Berlin. He conducted research in the fields of plasma physics, nonlinear optics, and laser physics and development. His current interests include applications of lasers and optical spectroscopy at the frontiers of science and medicine.

Katrin Kneipp received her Diploma and PhD degree in Physics and Dr sc in Physical Chemistry from Friedrich Schiller University in Jena, Germany. Her current research interests at Harvard Medical School include single-molecule and nanoscale spectroscopies and their broad interdisciplinary applications.

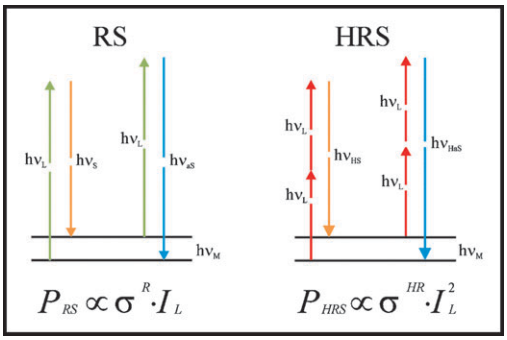

Fig. 1 Raman and hyper-Raman scattering in a molecular level scheme.

magnitude below typical two-photon fluorescence cross sections prevent the use of HRS as practical spectroscopic tool.

However, spectroscopic effects can be strongly affected when they take place in the immediate vicinity of metal surfaces and nanostructures due to coupling to surface plasmons.[5,6] In surface enhanced Raman scattering (SERS)[7–9] resonances between optical fields and surface plasmons lead to strongly enhanced Raman scattering signals of molecules in the vicinity of metal nanostructures.[10–18] SERS at extremely high enhancement level brings the effective Raman cross section to a level of fluorescence cross sections and enables the measurement of Raman spectra from single molecules.[19,20] In SERS, the dimension of the probed volume is determined by the confinement of the local optical field and can be two orders of magnitude smaller than the limit of $\sim\lambda/2$, which can be achieved in a confocal setup in normal spectroscopy.[21] So-called tip-enhanced Raman spectroscopy (TERS) is using highly confined probed volumes in combination with scanning probe microscopy and allows to acquire vibrational spectra along with corresponding topographic profiles at nanoscale resolution.[22,23]

Local optical fields also provide the key effect for the observation of so-called surface enhanced hyper-Raman scattering (SEHRS).[24] SEHRS benefits even to a greater extent from the high local optical fields than SERS, because of its non-linear dependence on the (enhanced) excitation field.[25]

This article reviews SERS at the single-molecule level and the potential and capabilities of the effect in bioanalytics. Since its early days, SERS was particularly appealing in the field of biophysics and biochemistry and several reviews are devoted to this topic.[26–31] Therefore, this article will mainly review applications of SERS in biomedical spectroscopy performed within the recent half decade.

After a brief introduction into the physics behind SERS at extremely high enhancement level and single-molecule Raman detection in Section 2, Section 3 discusses applications of SERS in bioanalytics including a new generation of labels based on SERS signals, sensitive detection and monitoring of biomolecules, and chemical probing in single live cells. Section 4 extends the concept of SERS to two-photon excitation by exploiting SEHRS.

2 SERS at extremely high enhancement level

2.1 Physics behind SERS

Fig. 2 gives a schematic of surface enhanced Raman scattering.

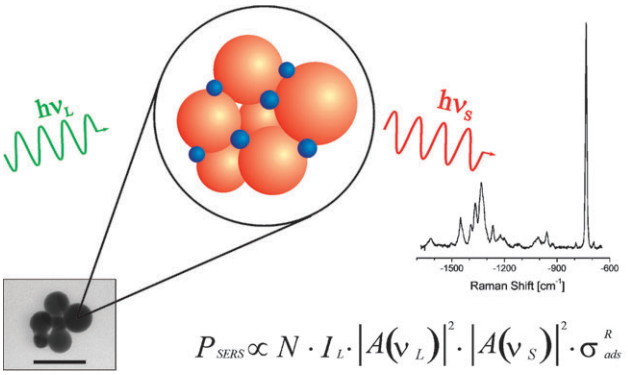

Fig. 2 Schematic of surface enhanced Raman scattering. The SERS spectrum shown as example was collected from 10^{-9} M adenine in a solution of silver nanoaggregates (adapted from ref. 18).

Molecules (blue dots) are attached to metal nanoparticles (orange balls); see the electron micrograph of colloidal gold particles. In analogy to normal Raman scattering, the SERS signal P^{SERS} depends on excitation intensity I_L and an effective SERS cross section $\sigma_{eff}^{SERS} = \sigma_{ads}^{R} A(\nu_L)^2 A(\nu_S)^2$, which benefits from the electromagnetic enhancement described by field enhancement factors $A(\nu_L)$, $A(\nu_S)$ for the excitation and scattered field and a chemical SERS effect, described by an increased Raman cross section σ_{ads}^{R} of the adsorbed molecule compared to the cross section in a "normal" Raman experiment σ^{R}. N is the number of molecules involved in the SERS process.

Electromagnetic field enhancement exists due to resonances of the optical fields with surface plasmons.[32,33] This leads to a redistribution of field intensities in the vicinity of nanoparticles resulting in areas of enhanced excitation intensities for the Raman process. Additionally, based on the same resonance mechanism, nanostructures can be considered as nanoantennae for transmitting and enhancing Raman scattered light. Electromagnetic field enhancement depends on the resonance process between plasmons and excitation and scattered fields, *e.g.* on morphology and material of the metal nanostructures and on excitation wavelengths of Raman scattering. A very simple electrostatic model describes already important properties of the electromagnetic SERS enhancement: It explains that silver, gold and copper are the best metals for SERS as they fulfill the plasmon resonance condition in the visible and near infrared range and have in this range also small imaginary parts of ε. It also shows that the enhancement is particularly strong when both excitation and scattered fields are in resonance with the surface plasmons. In general, the shift in frequencies between excitation and scattered light is small compared to the width of the plasmon resonance. Therefore, laser and Raman scattered field gain approximately the same due to field enhancement ($A(\nu_L) \sim A(\nu_S)$) and the electromagnetic SERS enhancement factor scales roughly with the fourth power of the enhancement of the amplitudes of local optical fields.

Chemical or electronic enhancement (in Fig. 1 $\sigma_{ads}^{R}/\sigma^{R}$) includes effects associated with an electronic coupling between molecule and metal.[10,34–39] For example, contributions of the metal may alter the Raman cross section of the

molecule–metal system compared to that of a free molecule leading to more efficient Raman scattering.[35,39] A very interesting electronic mechanism based on ballistic electrons and holes which are generated in the metal and which couple to the molecular orbitals, has been suggested since the early days of SERS,[10,34] and has been recently discussed again.[37] This model explains SERS as vibrationally inelastic tunnelling of ballistic electrons to the lowest unoccupied molecular orbital (LUMO) of the chemisorbed molecule. The return of the electron to its initial state leads to a strong emission of Raman shifted photons. All charge transfer processes are critical to the relative energy of the HOMO and LUMO in the SERS molecule with respect to the Fermi level in the metal and could explain the dependence of the SERS enhancement on the electrode potential and also differences in SERS enhancement factors for different molecules.

Field enhancement factors multiply chemical SERS enhancement.

An interesting question is the size of the total SERS enhancement factor. The effect of population pumping of vibrational levels due to a spontaneous Raman process observed in SERS identified unexpectedly large effective SERS cross sections on the order of at least 10^{-16} cm^2 per molecule. Such cross sections, which were inferred for near infrared (NIR) excitation that was not in resonance with electronic transitions in the target molecule, imply SERS enhancement factors of about fourteen orders of magnitude in order to overcome the gap to non-resonant Raman cross sections of 10^{30}–10^{29} cm^2. The studies also showed that only very few molecules of those present in the probed volume, are involved in the SERS process at such a high enhancement level.[40] This level of enhancement was also confirmed in straightforward experiment by comparing the non-resonant surface enhanced Raman signals of single molecules and the ''normal'' Raman signals of 10^{14} methanol molecules.[19,41]

Electromagnetic and/or chemical effects could account for the observed enhancement level on the order of 10^{14}. However, many experimental observations available so far provide evidence that electromagnetic enhancement based on plasmon resonances gives the mostly important contribution to high SERS enhancement. This is particularly supported by the fact that high levels of enhancement are always related to specific morphologies of nanostructures. Almost all reports on single-molecule Raman scattering rely on clusters or aggregates formed by individual silver or gold nanoparticles.[19,37,41–44]

Spatially-isolated silver nanoparticles exhibited enhancement factors on the order of 10^6, in agreement with theoretical estimates.[45] Our experimental results confirm that SERS enhancement factors can be on the order of 10^{14} for NaCl-activated silver colloidal aggregates or clusters formed by these nanoparticles. The strong enhancement factor of 10^{14} was found to be independent of the size of the colloidal clusters. In order to achieve consistency between the large effective SERS cross sections and the observed SERS Stokes signal, we have to come to the conclusion that molecules are involved in the SERS process at this extremely high enhancement at about 10^{-12} M concentration despite the 10^{-8} M concentration of the analyte in the SERS sample. Only a small fraction of the molecules in the sample exhibit a strong SERS enhancement. It might be interesting to note that 10^{-12} M is the same order of concentration as that of the 100–200-nm sized small colloidal clusters in the solution. That means that a small cluster offers excellent enhancement conditions for only 1–10 molecules. This number is too small for any correlation with ''chemically'' active sites associated with NaCl activation, for instance.[45]

Numerous theoretical estimates confirm high field enhancement in junctions between two silver or gold nanoparticles and for nanoparticle aggregates.[46–49] Particularly high enhancement occurs for fractal structures.[50–53] Enhancement factors of almost 10^{14} can result from the combination of local field enhancement associated with plasmon excitation and long range photonic interactions.[54] On the other hand, some studies come back to chemical mechanisms in order to explain extremely large SERS enhancement factors.[55] Still, the extent of electronic enhancement in SERS remains the subject of discussion.[44,56,57]

2.2 Single-molecule Raman scattering

SERS cross sections on the order of 10^{-16} cm^2 enable optical detection of single molecules. For target molecules showing no electronic transitions at the excitation wavelength, this requires SERS enhancement factors on the order of 10^{14}. For a strong resonance-Raman contribution of the target molecule in SERRS, the requirements for the surface enhancement effect in single-molecule Raman detection can be greatly lessened. For example, ''normal'' resonance-Raman scattering (RRS) that brings RRS cross sections to a level of about 10^{-25} cm^2, may lessen the requirement for SERS enhancement in single-molecule experiments to $\sim 10^9$.

One approach to single-molecule Raman measurements exploited extremely high nonresonant SERS cross sections obtained for silver and gold nanoaggregates at near-infrared excitation.[19,40–42]

Single-molecule Raman spectroscopy was also reported, based on surface enhanced resonance-Raman scattering (SERRS) using 514 nm excitation and rhodamine 6G adsorbed on silver nanoparticles as a target molecule.[20] Single-molecules detection was concluded from estimated numbers of molecules in the focal area and strong signal fluctuations and spectral changes that occurred in seconds on time scale.

Due to the confinement of extremely high SERS enhancement to nanoscale dimensions, it is possible to spectroscopically select ''a few'' or single molecules from a larger population and to measure SERS spectra, that exhibit single-molecule behavior, even when more molecules are present in the probed volume, since the SERS signal is dominated by single molecule(s) residing in the ''hottest spot''.[57–59] Although blinking had been claimed as a hallmark of single-molecule detection, power fluctuations and spectral changes in SERS spectra are not necessarily connected to single molecules and are inherently related to lower concentration ''many-molecule'' SERS.[60–62] Different effects can account for these observations, such as thermally and non-thermally activated diffusion of target molecules and/or impurities into and out of hot spots.[63]

Single-molecule Raman detection was proved by statistical analysis of SERS signals measured in time sequence in a SERS

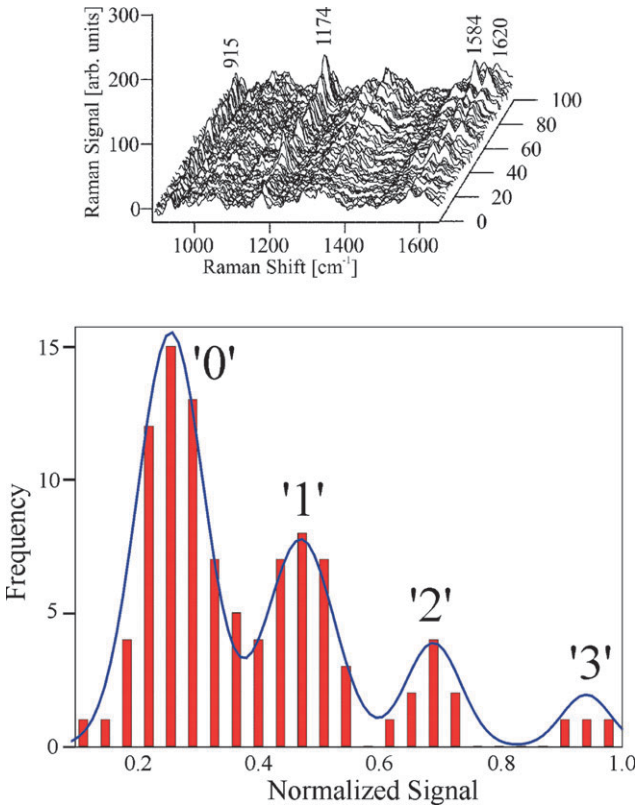

Fig. 3 100 SERS spectra (λ_{ex} = 830 nm) from single crystal violet-loaded silver nanoaggregates in solution collected in time sequence. Analyte concentrations of $\sim 10^{-14}$ M, which is $\sim$100 times lower than the concentrations of the nanoaggregates, ensures that statistically one out of hundred nanoaggregates carries a single analyte and that the average number of analytes in the probed volume is one or less. Below is the statistical distribution of the signals of the crystal violet line at 1175 cm^{-1} (adapted from ref. 19).

experiment using single analyte molecule-loaded silver nanoaggregates in solution.[19,41,42] When the average concentration of the target molecule in the probed volume is one molecule or less, Brownian motion of the metal nanoaggregates is moving single target molecules into and out of the probed volume leading to quantized scattering signals (Fig. 3). This reflects the probability to find 0, 1, 2 or 3 molecules in the probed volume during the actual measurement. The probability of observing 0, 1, 2 or 3 molecules is determined by a Poisson distribution corresponding the average number of molecules in the probed volume.

The change in the statistics of the Raman signal from Gaussian distribution, which is characteristic for many molecules to a Poisson distribution when the average number of target molecules in the scattering volume approaches one or fewer is evidence for single-molecule detection. Measurements performed at ten times higher concentration of the target molecule result in a Gaussian distribution of the scattering signals.[19,42]

Counting molecules based on quantized SERS signals for single molecules and Poisson statistics imply relatively uniform SERS enhancement factors for all target molecules.[19] Therefore, a Poisson distribution of single-molecule SERS signals can be observed only in SERS systems that avoid heterogeneity in the molecule–metal interactions and in SERS enhancement. This can be achieved in experiments on silver or gold nanoaggregates in solution with analyte concentrations $\ll$ concentration of the enhancing nanoaggregates as described in Fig. 3. Under these conditions, each single analyte molecule can find the "hottest spot" on "its own" nanoaggregate, where it is reasonable that the hottest spot on each nanoaggregate exhibit the same enhancement level. Experiments show, that hottest spots must have dimensions below 2 nm and that they provide an enhancement factor on the order of 10^{14}. Directing of single molecules to the hottest spots, most likely due to high field gradients, is one of the key questions in single-molecule detection based on SERS. So far, experiment performed at extremely low concentrations show that $\sim$80% of the molecules present in the solution find a place at the "hottest spot".[19,42]†

Recent SERRS experiments confirm single-molecule Raman detection by using spectral information of two different competing analyte molecules instead of signals strengths.[62] In the study, silver nanoaggregates were covered with a 1 : 1 mixture of two isotopologues of Rhodamine 6G, which are "absolutely equal" molecules regarding adsorption properties, but each of them offers unique vibrational signatures. Single-molecule behavior can be verified by tracking the spectral signature of the individual silver particles: When sufficiently low concentrations of both analyte molecules are introduced to a solution of silver nanoparticles such that, on average, only one type of molecule is adsorbed to each nanoparticle, each SERS spectrum contains spectral features of only a single isotopologue. On the other hand, as the coverage is increased such that both analytes should be present on a single nanoparticle, one should observe the vibrational characteristics of both analytes. Thus, one can distinguish single- *vs.* multi-molecule SERS by the number of peaks in the SERS spectrum (see also Fig. 4).

3 SERS in bioanalytics

There are several potential capabilities that make SERS a promising method in bioanalytics.[31] Most excitingly, the effect combines the high level of molecular structural information of a vibrational spectroscopy with ultrasensitive detection limits. This allows to detect molecules and to establish their structural identity in very small quantities down to the single-molecule level. Probed volumes at the nm opens the opportunity to probe small biological structures. Effective SERS cross sections on the level of fluorescence cross sections of good fluorophores along with spectral signatures composed from several narrow lines suggest optical labels based on SERS signals.[64,65] Compared to conventional fluorescence labels, SERS labels offer several advantages and have the potential to become the next-generation labelling technology for bioanalytics.

† It should be noted that our experiment is different from experiments carried out at the presence of a few hundred molecules[98] or in tip-enhanced SERS experiments.[99,100] Experimental conditions in these experiments prevent that the collected SERS signal is generated by single molecules that experience a relative uniform enhancement level.

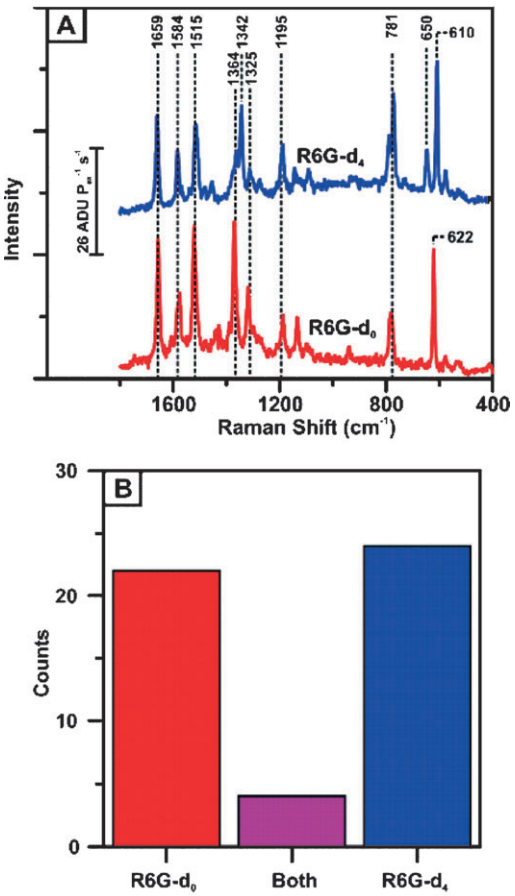

Fig. 4 Representative SERRS spectra (λ_{ex} = 532 nm) measured from two nanoaggregates in which it is evident that there is only one isotopologue of rhodamine 6G present on each. Below is the histogram of occurrences of the three most likely possible cases that R6G-*d*0, R6G-*d*4 or both molecules are present on the silver particle (reproduced with courtesy from ref. 62).

Gold nanoparticles or nanoaggregates probe chemistry in their local environment by delivering the enhanced Raman spectra of molecules in their vicinity and can serve as nanosensors to probe small biological structures such as cells and bacteria.[66–72]

In the following, we present some recent applications, in order to illustrate the above mentioned capabilities of SERS in bioanalytics.

3.1 SERS label

One interesting application of SERS in biomedical sensing includes SERS labels based on highly selective surface enhanced Raman spectrum of a reporter attached to an enhancing silver or gold nanostructure.[73–75] Additionally, the SERS tag can be functionalized using specific linker in order to target specific biomolecules or biological structures. Au or Ag cores functionalized with Raman active molecules can also be encapsulated in a glass shell, which provides the SERS label with mechanical and chemical stability.[76]

Distinguishable spectral signatures even for similar reporter molecules enable a large pool of spectrally non-overlapping labels. Since SERS works also well in the non-resonant regime, SERS labels do not suffer from photobleaching or self quenching. As SERS works also with non-resonant excitation, all labels can be used at the same excitation wavelength. Therefore, SERS labels benefit from real multiplexing capabilities, for example, in labeling and simultaneous identification of many different DNA strands.[74,75,77,78]

3.2 Ultrasensitive detection and monitoring of biomedically relevant molecules

To detect and to identify single molecules by fluorescence, in most cases, they must be labelled using fluorescence tags such as dye molecules or quantum dots to achieve high enough fluorescence quantum yields and distinguishable spectral properties. Alternatively to fluorescence, single biomolecules can be detected based on the spectral signature of a SERS tag or by their intrinsic surface enhanced Raman spectrum.[79] In general, SERS spectra, comprised of different vibrational modes, provide high structural information content on the target molecule, but also measuring only one typical SERS line and using this Raman line as a spectroscopic signature for the specific molecule is a useful tool for detecting a known molecule and for monitoring its distribution without the use of fluorescence labels.

Enkephalin, an endogeneous substance in the human brain showing morphine-like biological functions, has been detected at the single-molecule level based on the surface-enhanced Raman signal of the ring breathing mode of phenylalanine, which is one building block of the molecule. For enhancing the Raman signal, the enkephalin molecules were attached to silver colloidal cluster structures. The SERS signal of the strongly enhanced mode of phenylalanine can be used as intrinsic marker for detecting a single enkephalin molecule without the use of a specific label. The reported result suggests the use of the phenylalanine 1000 cm^{-1} SERS line as spectroscopic signature for monitoring single proteins containing this amino acid as a building block.[79]

As another example, gold nanoparticles were capped with a bifunctional molecule capable of forming a covalent link with the aromatic residues of the protein moiety. The typical vibrations of the diazo bond established between the bifunctional molecule and the target protein are found to be selectively enhanced by the conjugated gold nanoparticles, and therefore, constitutes a Raman marker. After the interaction of functionalized gold nanoparticles with antithrombin as a sensitive recognition element, immobilized on a capture substrate, the detection of thrombin was reported at a concentration of about 10^{-13} M.[80]

A particular challenge is to apply SERS in living systems and to real medical problems. A first *in vivo* application of SERS demonstrated quantitative *in vivo* glucose measurements from an animal model.[81] A SERS active structure was subcutaneously implanted in an animal such that the glucose concentration of the interstitial fluid could be measured by optically addressing the sensor through an optical window in the animal's body. The key questions in this application include the development of a stable and biocompatible SERS active substrate to ensure uniform and strong average enhancement and reversibly binding of glucose. Single-

molecule sensitivity is not required in this application, but a linear response of the SERS signal in the range of physiologically relevant glucose concentrations. The result of the study indicate that glucose binds reversibly to the SERS-active surface and that changes in concentration as rapid as 30 seconds can be spectroscopically measured.

3.3 Chemical probing in live cells

Gold nanoparticles have been tools of the trade in cell biology because of their favorable physical and chemical properties and biocompatibility. An exciting new aspect in their applications exploits gold nanoparticles as multifunctional SERS nanosensors. These mobile sensors can probe cellular chemistry at subendosomal resolution by delivering the enhanced Raman spectra of cellular molecules in their nanoenvironment.[66,71,82] Due to the large effective Raman scattering cross section, SERS probes fulfill the requirements of dynamic *in vivo* systems—the use of very low laser powers and very short data acquisition times. For example, gold nanoparticles have been used to directly probe the chemical composition of endosomes of different stages and for the detection of specific cellular molecules, such as adenosine monophosphate (AMP).[70] Gold or silver nanoparticles can serve in cells also as labels that highlight cellular structures based on the surface-enhanced Raman signature of a reporter molecule linked to them.[68,83,84]

Moreover, gold or silver nanoparticles with reporter molecules attached that exhibit a known and calibrated pH dependent SERS signature,[85–87] can act also as intracellular pH probe.[72,88] Determining and monitoring pH in cells and cellular compartments is of particular importance for a better understanding of a broad range of physiological and metabolic processes. Fig. 5 demonstrates pH imaging in single live cells at subendosomal resolution using SERS nanosensors.

4 Extension of SERS to two-photon excitation

Two-photon excitation is gaining rapidly in interest and significance in spectroscopy and microscopy. For biological applications, the greatly reduced possible phototoxicity and stress to the sample due to longer wavelengths excitation, as well as the confinement of the two-photon interaction to the focus of the laser beam are major advantages over one-photon methods.[89,90] The development of optical methods that are suitable for two-photon excitation is therefore an important task in advancing optical techniques for biological applications.

Hyper-Raman scattering (HRS) (see Fig. 1) is a potential tool for two-photon excited vibrational spectroscopy. HRS follows symmetry selection rules different from regular one-photon RS, and therefore the spectral information obtained in HRS can be complementary to the information from RS. Surface enhanced hyper-Raman scattering (SEHRS) is analogous to the enhancement of one-photon-excited Raman signals in SERS. SEHRS has been demonstrated since the early days of SERS.[24] Small aggregates, consisting of gold and silver nanoparticles and fractal structures of these metals that provide extremely strong field enhancement, can give rise to enhancement factors for HRS signals up to 20 orders of magnitude.[91] The strong field enhancement can compensate for the extremely small cross section of HRS and allows the measurement of SEHRS spectra at excitation intensities of 10^6–10^7 W cm^{-2}, conditions that can be easily achieved with mode-locked picosecond lasers under weak focusing conditions[92] but also in tightly focused continuous wave (cw)[93] or low-energy pulsed lasers.[94]

Effective cross sections of SEHRS have shown to be on the order of 10^{-46}–10^{-45} cm^{4}s, comparable or even better than the best cross sections for two-photon fluorescence obtained so far.[25] This suggests versatile optical SERS/SEHRS labels suitable for both one- and two-photon excitation. Fig. 6 shows

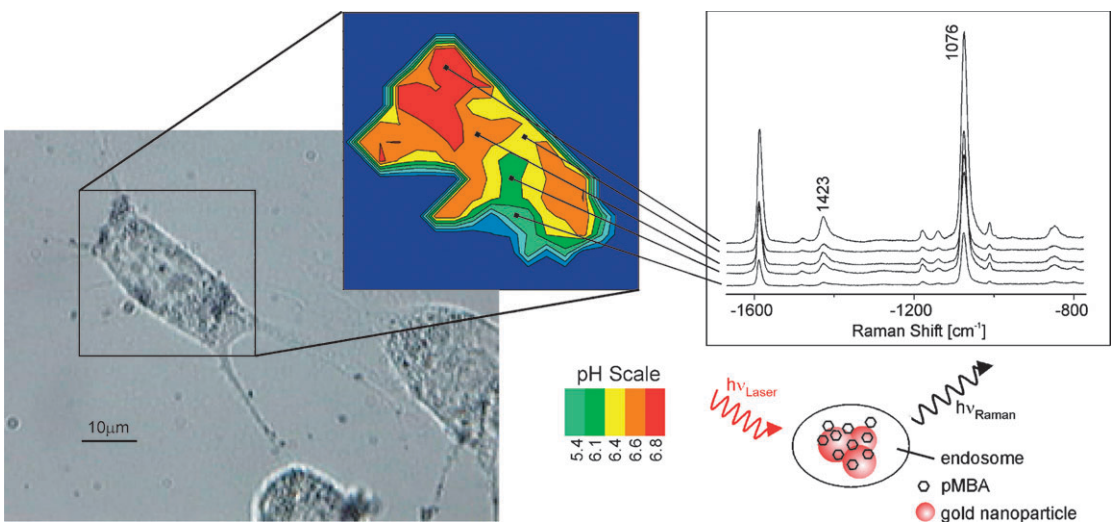

Fig. 5 Probing and imaging pH values in single live cells using a SERS nanosensor, which exploits the pH sensitive SERS spectrum of 4-mercaptobenzoic acid (pMBA) on gold nanoaggregates. (a) Photomicrograph of an NIH/3T3 incubated with the pMBA gold nanosensors. (b) pH map of the cell shown as false color plot of the pH sensitive ratios of the SERS lines (c) SERS spectra collected in the cellular compartments exhibiting different pH (reproduced with courtesy from ref. 72).

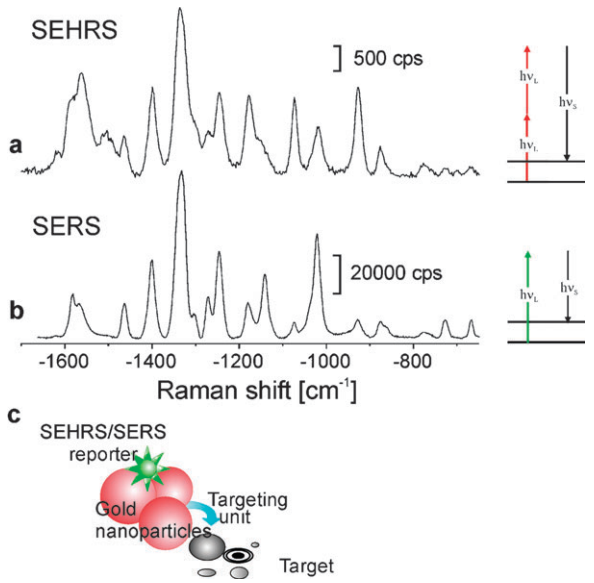

Fig. 6 SEHRS (a) and SERS (b) spectra of 10^{-8} M Rose Bengal on silver nanoaggregates. For this molecule, RS and HRS spectrum show the same modes. Two-photon excited SEHRS spectra were measured using 1064 nm mode locked ps pulses. One-photon excited SERS spectra were collected using 785 nm cw light (c) schematic of a SERS/SEHRS label (reproduced with courtesy from ref. 25)

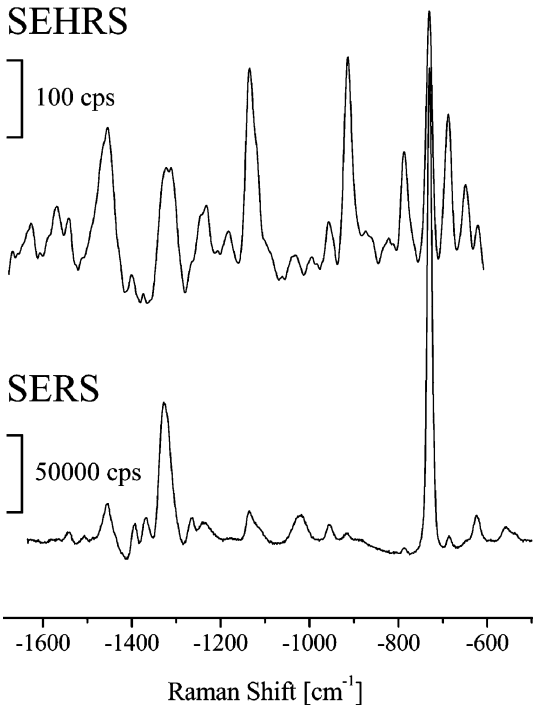

Fig. 7 SEHRS and SERS spectra of 10^{-6} M adenine in aqueous solution with silver nanoaggregates. One-photon excited SERS spectra were measured using 514.5 nm cw light, intensity 7×10^{22} photons cm^{-2} s^{-1}. Two-photon excited SEHRS spectra were measured using 1064 nm mode locked ps pulses (7 ps, 78 MHz repetition rate, triangle pulse shape), intensity 9×10^{26} photons cm^{-2} s^{-1} (reproduced with courtesy from ref. 25).

the schematic of a SEHRS/SERS label along with its spectral signature. *e.g.* SEHRS and SERS spectra of the "reporter dye" Rose Bengal.

Extremely strong SEHRS signals are also obtained for adenine, at two-photon excitation with 1064 nm laser light (see Fig. 7). Compared to the SERS spectrum of adenine its SEHRS spectrum shows several additional strong scattering lines that can be ascribed to IR-active vibrations.[95] Adenine absorbs in the UV spectral region, and hence SEHRS cannot benefit from any one- or two-photon molecular electronic resonance contribution. The example of adenine illustrates, that effective SEHRS cross sections can exceed by far the two-photon fluorescence cross sections encountered for common biomolecules.[96]

High effective two-photon cross sections as well as additional information on the vibrational spectrum of a molecule make SEHRS a promising two-photon spectroscopic tool for molecular structural probing.

5 Conclusion

Despite controversy on the origin of the enhancement, there seems to be no doubt on the existence of effective SERS cross sections on the order of 10^{-16} cm^2, *e.g.* cross sections that enable optical detection of single molecules. Most molecules display unique Raman features whereas far less molecules show fluorescence. Due to the primarily electromagnetic origin of the enhancement of the Raman signal, it should be possible to achieve an equally strong SERS effect for each molecule, thus making SERS a single-molecule tool for a broad range of molecules.

Another interesting aspect of SERS for single-molecule detection involves the total number of photons that can be emitted by a molecule, which is determined by the maximum number of excitation-emission cycles a molecule survives. Compared to fluorescence, SERS avoids or strongly reduced photodecomposition. Another number that is of particular interest for the rapid detection and screening of single molecules is the maximum number of photons that can be emitted by a molecule per time interval. Under saturation conditions, this number is inversely proportional to the lifetime of the excited molecular states involved in the optical detection process. Due to the shorter vibrational relaxation times as compared to the electronic relaxation times, a molecule can go through more Raman cycles than fluorescence cycles per time interval. Therefore, the number of Raman photons per time interval that can be emitted by a molecule under saturation conditions can be higher than the number of fluorescence photons by a factor of 10^2 to 10^3.[97]

Structurally selective detection of single molecules and quantification of matter by counting single molecules represent the ultimate limit in chemical analysis and trace detection. Counting of singe molecules requires a uniform level of highest SERS enhancement and directing single molecules to these "hottest spots".

Extremely high enhancement of surface enhanced hyper-Raman scattering allows successful extension of SERS-based concepts in spectroscopy to two-photon excitation. The approach suggests highly efficient two-photon labels based on the SEHRS signature of a reporter molecule on gold- or silver nanoaggregates as well as two-photon vibrational

spectroscopy, where the SEHRS spectrum can provide additional structural information. For non-destructive chemical probing, SEHRS combines the advantages of two-photon spectroscopy with the structural information of vibrational spectroscopy, and the high sensitivity and nanometer-scale local confinement of plasmonics-based spectroscopy.

A big challenge in all basic studies and applications is control of SERS enhancement. So far, best enhancement factors are experimentally observed for random SERS systems formed by nature, such as aggregates of gold and silver nanoparticles. Further development in nanotechnology will enable us to build such nanostructures in a controlled way and to probe these structures with nm resolution using one- and multiphoton excitation. In addition to "nanoscale" design between 10 and 100 nm, which controls the electromagnetic enhancement, electronic and "atomic scale" properties will be important in order to control also the "electronic " contribution to the enhancement as well as binding, and potential wandering and release of target molecules.

Overall, SERS at extremely high enhancement level transforms Raman spectroscopy from a structural analytical tool to a structurally sensitive single molecule and nanoscale probe, suitable for one- and two-photon excitation. Exciting applications demonstrate the potential of the method, particularly also in biospectroscopy.

References

1 C. V. Raman and K. S. Krishnan, *Nature*, 1928, **121**, 501.
2 G. Landsberg and L. Mandelstam, *Naturwissenschaften*, 1928, **16**, 557.
3 V. N. Denisov, B. N. Mavrin and V. B. Podobedov, *Phys. Rep.*, 1987, **151**, 1.
4 R. L. McCreery, in *Modern Techniques in Raman Spectroscopy*, ed. J. J. Laserna, John Wiley & Sons, Chichester–New York–Brisbane–Toronto–Singapore, 1996, p. 446.
5 K. A. Willets and R. P. Van Duyne, *Annu. Rev. Phys. Chem.*, 2007, **58**, 267–297.
6 S. Lal, S. Link and N. J. Halas, *Nat. Photonics*, 2007, **1**, 641–648.
7 M. Fleischman, P. J. Hendra and A. J. McQuillan, *Chem. Phys. Lett.*, 1974, **26**, 123.
8 D. L. Jeanmaire and R. P. V. Duyne, *J. Electroanal. Chem.*, 1977, **84**, 1–20.
9 M. G. Albrecht and J. A. Creighton, *J. Am. Chem. Soc.*, 1977, **99**, 5215–5217.
10 A. Otto, in *Light Scattering in Solids IV. Electronic Scattering, Spin Effects, SERS and Morphic Effects*, ed. M. Cardona and G. Guntherodt, Springer-Verlag, Berlin, Germany, 1984, pp. 289–418.
11 M. Moskovits, *Rev. Mod. Phys.*, 1985, **57**, 783–826.
12 K. Kneipp, *Exp. Tech. Phys.*, 1990, **38**, 3–28.
13 A. Campion and P. Kambhampati, *Chem. Soc. Rev.*, 1998, **27**, 241–250.
14 K. Kneipp, H. Kneipp, I. Itzkan, R. R. Dasari and M. S. Feld, *Chem. Rev.*, 1999, **99**, 2957–2975.
15 C. L. Haynes, C. R. Yonzon, X. Y. Zhang and R. P. Van Duyne, *J. Raman Spectrosc.*, 2005, **36**, 471–484.
16 K. Kneipp, H. Kneipp and J. Kneipp, *Acc. Chem. Res.*, 2006, **39**, 443–450.
17 *Surface Enhanced Raman Scattering – Physics and Applications*, ed. K. Kneipp, M. Moskovits and H. Kneipp, Springer, Heidelberg–Berlin–New York, 2006.
18 K. Kneipp, *Phys. Today*, 2007, **60**, 40–46.
19 K. Kneipp, Y. Wang, H. Kneipp, L. T. Perelman, I. Itzkan, R. R. Dasari and M. S. Feld, *Phys. Rev. Lett.*, 1997, **78**, 1667.
20 S. Nie and S. R. Emory, *Science*, 1997, **275**, 1102–1106.
21 K. Kneipp, H. Kneipp, P. Corio, S. D. M. Brown, K. Shafer, J. Motz, L. T. Perelman, E. B. Hanlon, A. Marucci, G. Dresselhaus and M. S. Dresselhaus, *Phys. Rev. Lett.*, 2000, **84**, 3470–3473.
22 R. M. Stockle, S. Yung Doug, V. Deckert and R. Zenobi, *Chem. Phys. Lett.*, 2000, **318**, 131–136.
23 A. Hartschuh, E. J. Sanchez, X. S. Xie and L. Novotny, *Phys. Rev. Lett.*, 2003, **90**, 095503-1–095503-4.
24 D. V. Murphy, K. U. Von Raben, R. K. Chang and P. B. Dorain, *Chem. Phys. Lett.*, 1982, **85**, 43–47.
25 J. Kneipp, H. Kneipp and K. Kneipp, *Proc. Natl. Acad. Sci. USA*, 2006, **103**, 17149–17153.
26 T. M. Cotton, Jae-Ho Cotton and G. D. Chumanov, *J. Raman Spectrosc.*, 1991, **22**, 729–742.
27 E. Koglin and J. M. Sequaris, *Top. Curr. Chem.*, 1986, **134**, 1.
28 R. F. Paisley and M. D. Morris, *Prog. Anal. Spectrosc.*, 1988, **11**, 111–140.
29 K. Kneipp, H. Kneipp, I. Itzkan, R. R. Dasari and M. S. Feld, *Curr. Sci.*, 1999, **77**, 915–924.
30 T. Vo-Dinh, D. L. Stokes, G. D. Griffin, M. Volkan, U. J. Kim and M. I. Simon, *J. Raman Spectrosc.*, 1999, **30**, 785–793.
31 K. Kneipp, H. Kneipp, I. Itzkan, R. R. Dasari and M. S. Feld, *J. Phys.: Condens. Matter*, 2002, **14**, R597–R624.
32 D. S. Wang and M. Kerker, *Phys. Rev. B: Condens. Matter Mater. Phys.*, 1981, **24**, 1777–1790.
33 M. Moskovits, L. Tay, J. Yang and T. Haslett, *ICORS 2000*, 2000.
34 B. N. J. Persson, *Chem. Phys. Lett.*, 1981, **82**, 561–565.
35 J. R. Lombardi, R. L. Birke, L. Tianhong and X. Jia, *J. Chem. Phys.*, 1986, **84**, 4174–4180.
36 P. Kambhampati, C. M. Child, M. C. Foster and A. Campion, *J. Chem. Phys.*, 1998, **108**, 5013–5026.
37 A. M. Michaels, J. Jiang and L. Brus, *J. Phys. Chem. B*, 2000, **104**, 11965–11971.
38 B. N. J. Persson, K. Zhao and Z. Y. Zhang, *Phys. Rev. Lett.*, 2006, **96**, 207401.
39 J. R. Lombardi and R. L. Birke, *J. Chem. Phys.*, 2007, **126**, 244709.
40 K. Kneipp, Y. Wang, H. Kneipp, I. Itzkan, R. R. Dasari and M. S. Feld, *Phys. Rev. Lett.*, 1996, **76**, 2444.
41 K. Kneipp, H. Kneipp, G. Deinum, I. Itzkan, R. R. Dasari and M. S. Feld, *Appl. Spectrosc.*, 1998, **52**, 175–178.
42 K. Kneipp, H. Kneipp, V. B. Kartha, R. Manoharan, G. Deinum, I. Itzkan, R. R. Dasari and M. S. Feld, *Phys. Rev. E*, 1998, **57**, R6281–6284.
43 H. X. Xu, E. J. Bjerneld, M. Kall and L. Borjesson, *Phys. Rev. Lett.*, 1999, **83**, 4357–4360.
44 A. M. Michaels, M. Nirmal and L. E. Brus, *J. Am. Chem. Soc.*, 1999, **121**, 9932–9939.
45 K. Kneipp and H. Kneipp, *Isr. J. Chem.*, 2006, **46**, 299–305.
46 M. Inoue and K. Ohtaka, *J. Phys. Soc. Jpn.*, 1983, **52**, 3853–3864.
47 H. X. Xu, J. Aizpurua, M. Kall and P. Apell, *Phys. Rev. E*, 2000, **62**, 4318–4324.
48 P. Nordlander, C. Oubre, E. Prodan, K. Li and M. I. Stockman, *Nano Lett.*, 2004, **4**, 899–903.
49 M. Moskovits, L. L. Tay, J. Yang and T. Haslett, in *Optical Properties of Nanostructured Random Media*, Springer-Verlag, Berlin, 2002, vol. 82, pp. 215–226.
50 M. I. Stockman, V. M. Shalaev, M. Moskovits, R. Botet and T. F. George, *Phys. Rev. B*, 1992, **46**, 2821–2830.
51 K. R. Li, M. I. Stockman and D. J. Bergman, *Phys. Rev. Lett.*, 2003, **91**, 227402.
52 Z. J. Wang, S. L. Pan, T. D. Krauss, H. Du and L. J. Rothberg, *Proc. Natl. Acad. Sci. USA*, 2003, **100**, 8638–8643.
53 M. Stockman, Surface-Enhanced Raman Scattering: Physics and Applications, *Top. Appl. Phys.*, 2006, **103**, 47–66.
54 S. L. Zou and G. C. Schatz, *Chem. Phys. Lett.*, 2005, **403**, 62–67.
55 L. P. Capadona, J. Zheng, J. I. Gonzalez, T. H. Lee, S. A. Patel and R. M. Dickson, *Phys. Rev. Lett.*, 2005, **94**, 058301.
56 A. Otto, *J. Raman Spectrosc.*, 2005, **36**, 497–509.
57 D. P. Fromm, A. Sundaramurthy, A. Kinkhabwala, P. J. Schuck, G. S. Kino and W. E. Moerner, *J. Chem. Phys.*, 2006, **124**, 061101.
58 A. R. Bizzarri and S. Cannistraro, *Appl. Spectrosc.*, 2002, **56**, 1531–1537.

59 P. J. G. Goulet and R. F. Aroca, *Anal. Chem.*, 2007, **79**, 2728–2734.
60 C. J. L. Constantino, T. Lemma, P. A. Antunes and R. Aroca, *Anal. Chem.*, 2001, **73**, 3674–3678.
61 P. C. Andersen, M. L. Jacobson and K. L. Rowlen, *J. Phys. Chem. B*, 2004, **108**, 2148–2153.
62 J. A. Dieringer, R. B. Lettan, K. A. Scheidt and R. P. VanDuyne, *J. Am. Chem. Soc.*, 2007, **129**, 16249–16256.
63 A. Weiss and G. Haran, *J. Phys. Chem. B*, 2001, **105**, 12348–12354.
64 W. E. Doering, M. E. Piotti, M. J. Natan and R. G. Freeman, *Adv. Mater.*, 2007, **19**, 3100–3108.
65 T. Vo-Dinh, L. R. Allain and D. L. Stokes, *J. Raman Spectrosc.*, 2002, **33**, 511–516.
66 J. Kneipp, Surface-Enhanced Raman Scattering: Physics and Applications, *Top. Appl. Phys.*, 2006, **103**, 335–349.
67 L. Zeiri, B. V. Bronk, Y. Shabtai, J. Eichler and S. Efrima, *Appl. Spectrosc.*, 2004, **58**, 33–40.
68 J. Kneipp, H. Kneipp, W. L. Rice and K. Kneipp, *Anal. Chem.*, 2005, **77**, 2381–2385.
69 W. R. Premasiri, D. T. Moir, M. S. Klempner, N. Krieger, G. Jones and L. D. Ziegler, *J. Phys. Chem. B*, 2005, **109**, 312–320.
70 J. Kneipp, H. Kneipp, M. McLaughlin, D. Brown and K. Kneipp, *Nano Lett.*, 2006, **6**, 2225–2231.
71 R. J. Dijkstra, W. Scheenen, N. Dam, E. W. Roubos and J. J. ter Meulen, *J. Neurosci. Methods*, 2007, **159**, 43–50.
72 J. Kneipp, H. Kneipp, B. Wittig and K. Kneipp, *Nano Lett.*, 2007, **103**, 17149–17153.
73 L. R. Allain and T. Vo-Dinh, *Anal. Chim. Acta*, 2002, **469**, 149–154.
74 Y. C. Cao, R. C. Jin, J. M. Nam, C. S. Thaxton and C. A. Mirkin, *J. Am. Chem. Soc.*, 2003, **125**, 14676–14677.
75 Y. W. C. Cao, R. C. Jin and C. A. Mirkin, *Science*, 2002, **297**, 1536–1540.
76 S. P. Mulvaney, M. D. Musick, C. D. Keating and M. J. Natan, *Langmuir*, 2003, **19**, 4784–4790.
77 K. Faulds, W. E. Smith and D. Graham, *Anal. Chem.*, 2004, **76**, 412–417.
78 L. Qin, M. J. Banholzer, J. E. Millstone and C. A. Mirkin, *Nano Lett.*, 2007, **7**, 3849–3853.
79 K. Kneipp, H. Kneipp, S. Abdali, R. W. Berg and H. Bohr, *Spectrosc.–Int. J.*, 2004, **18**, 433–440.
80 A. R. Bizzarri and S. Cannistraro, *Nanomed. Nanotechnol. Biol. Med.*, 2007, **3**, 306–310.
81 A. D. Stuart, J. M. Yuen, N. C. Shah, O. Lyandres, C. R. Yonzon, M. R. Glucksberg, J. T. Walsh and R. P. Van Duyne, *Anal. Chem.*, 2006, **78**, 7211–7215.
82 A. Shamsaie, M. Jonczyk, J. Sturgis, J. P. Robinson and J. Irudayaraj, *J. Biomed. Opt.*, 2007, **12**, 020502.
83 M. B. Wabuyele, F. Yan, G. D. Griffin and T. Vo-Dinh, *Rev. Sci. Instrum.*, 2005, **76**, 063710-1–063710-7.
84 Y. Wang, D. Li, P. Li, W. Wang, W. Ren, S. Dong and E. Wang, *J. Phys. Chem. C*, 2007, **111**, 16833–16839.
85 A. Michota and J. Bukowska, *J. Raman Spectrosc.*, 2003, **34**, 21–25.
86 S. W. Bishnoi, C. J. Rozell, C. S. Levin, M. K. Gheith, B. R. Johnson, D. H. Johnson and N. J. Halas, *Nano Lett.*, 2006, **6**, 1687–1692.
87 A. M. Schwartzberg, T. Y. Oshiro, J. Z. Zhang, T. Huser and C. E. Talley, *Anal. Chem.*, 2006, **78**, 4732–4736.
88 C. E. Talley, L. Jusinski, C. W. Hollars, S. M. Lane and T. Huser, *Anal. Chem.*, 2004, **76**, 7064–7068.
89 W. R. Zipfel, R. M. Williams and W. W. Webb, *Nat. Biotechnol.*, 2003, **21**, 1369–1377.
90 P. T. C. So, C. Y. Dong, B. R. Masters and K. M. Berland, *Annu. Rev. Biomed. Eng.*, 2000, **2**, 399–429.
91 K. Kneipp, H. Kneipp, I. Itzkan, R. R. Dasari and M. S. Feld, *Chem. Phys.*, 1999, **247**, 155–162.
92 H. Kneipp, K. Kneipp and F. Seifert, *Chem. Phys. Lett.*, 1993, **212**, 374–378.
93 T. Itoh, Y. Ozaki, H. Yoshikawa, T. Ihama and H. Masuhara, *Appl. Phys. Lett.*, 2006, **88**, 084102.
94 L. Weinan and A. Meyers-Kelley, *J. Am. Chem. Soc.*, 2006, **128**, 3492–3493.
95 B. Schrader, *Raman/Infrared Atlas of Organic Compounds*, VCH Publishers, Weinheim, 1989.
96 C. Xu, W. R. Zipfel, J. B. Shear, R. M. Williams and W. W. Webb, *Proc. Natl. Acad. Sci. USA*, 1996, **93**, 10763–10768.
97 K. Kneipp, *Exp. Tech. Phys.*, 1988, **36**, 161–166.
98 P. G. Etchegoin, M. Meyer and E. C. Le Ru, *Phys. Chem. Chem. Phys.*, 2007, **9**, 3006–3010.
99 W. H. Zhang, B. S. Yeo, T. Schmid and R. Zenobi, *J. Phys. Chem. C*, 2007, **111**, 1733–1738.
100 K. F. Domke, D. Zhang and B. Pettinger, *J. Phys. Chem. C*, 2007, **111**, 8611–8616.

